AEROELASTIC ANALYSIS OF WIND ENERGY CONVERSION SYSTEMS

John Dugundji

Department of Aeronautics and Astronautics
Massachusetts Institute of Technology
Cambridge, Massachusetts 02139

ABSTRACT

An aeroelastic investigation of horizontal axis wind turbines is described. The study is divided into two simpler areas, namely, the aeroelastic stability of a single blade on a rigid tower, and the mechanical vibrations of the rotor system on a flexible tower. Some resulting instabilities and forced vibration behavior are described.

INTRODUCTION

The aeroelastic analysis of horizontal axis wind turbines may be divided into two convenient areas, namely, (a) the investigation of the aeroelastic stability and response of a single blade on a rigid tower, and (b) the investigation of the mechanical stability and vibrations of the rotor system on a flexible tower. With a reasonable understanding of the behavior in these two areas, the more complex problem involving a completely coupled blade-tower aeroelastic system can be better understood.

The present report deals with some work performed for ERDA in the two areas cited above. The aim has been to investigate the basic mechanisms and to reduce these analyses to forms in which they can be readily used for trade-off analyses.

AEROELASTIC STABILITY OF SINGLE BLADE

Using the equivalent hinge concept, the nonlinear equations of motion were written for large deflections of a rigid blade, with elastic hinges at the root, rotating about a rigid tower. The blade was assumed to have a flapping (β), lagging (ϕ), and feathering (θ) degree of freedom, and the effects of preconing of the blade relative to the feathering hinge (δ), and of the feathering hinge relative to the plane of rotation (β_H), were included. Quasi-steady aerodynamic forces were assumed. The equations were first solved to obtain the static, steady state displacement in flap (β_0) and lag (ϕ_0). Then the equations of motion were linearized by assuming small perturbations about the steady state flap and lag displacements found above. The resulting linear equations take the form

$$[A]\{\ddot{x}\} + [D]\{\dot{x}\} + [K]\{x\} = 0 \qquad (1)$$

where {x} represents the perturbation displacements in β, ϕ, θ and [A], [D], [K] represent the 3x3 mass, damping, and stiffness matrices respectively. These equations were investigated for stability by recasting them as standard first order equations, and extracting the eigenvalues $p_n = a_n + i\ b_n$ using standard procedures. The resulting a_n's indicate the damping characteristics, and the b_n's the frequencies of the resulting oscillations.

A wide range of parametric variations are being investigated. Figure 1 shows some typical results from this analysis showing effects of preconing on the stability margins. The results are presented in the form of modal critical damping ratio $\zeta \approx -a_n/b_n$ since it is believed this more clearly indicates the strength of the instability (or stability) than simple stability boundaries. It is seen here that positive droop angles (δ) can particularly decrease the stability margin.

The analyses described above have been based on equivalent hinges in order to provide a rapid and reasonably accurate tool for predicting stability characteristics. However, a more elaborate program is being developed which allows for distributed flexibility of all three hinges, and this program will be used to validate the results using equivalent hinges.

The linear aeroelastic stability analyses have been supplemented by some nonlinear, large deflection analyses again using equivalent hinges, to determine the nonlinear limit cycle behavior of these instabilities. The harmonic balance method was applied and the resulting nonlinear equations were solved by the Newton-Raphson technique. Both the self-excited aeroelastic instabilities and the dynamic response to gravity and wind shear loads were investigated. Figure 2 shows the nonlinear limit cycle behavior of a predominantly flapping-torsion type instability as rotation speed Ω is increased. The nonlinearity tends to be of a softening type, i.e., steady limit cycles can occur somewhat below the linear critical rotation speed if a large enough disturbance is given to the system.

MECHANICAL VIBRATIONS OF ROTOR-TOWER SYSTEM

The mechanical instabilities and vibrations that may result from the interaction of the flexible rotating blades with the base motions of the supporting tower were also investigated. The simplest of these interactions involves the coupling of the tower side motions (q_L) with the blade lagging motions (ϕ), which can give rise to a strong mechanical instability (the "gound resonance" effect of helicopters), as well as significant forced vibration effects due to blade unbalance and gravity forces. Using the equivalent hinge concept, the equations of motion for small vibrations of such a rotor-tower system are

$$M_L\ddot{q}_L + c_L\dot{q}_L + k_1 q_1 + \overset{i}{\underset{i}{\Sigma}}\ S_i\frac{d^2}{dt^2}(\phi_i\cos\psi_i) = \Omega^2\ \overset{i}{\underset{i}{\Sigma}}\ S_i\sin\ \psi_i$$

$$S_i\cos\psi_i\ \ddot{q}_L + I_i\ddot{\phi}_i + c_\phi\dot{\phi}_i + k_\phi\phi_i = g[S_i\sin\psi_i + S_i\phi_i\cos\psi_i]$$

$$i = 1,2,\ldots N \qquad\qquad (2)$$

54

where $\psi_i = \Omega t + 2\pi(i-1)/N$ represents the angular position of the ith blade, g is the acceleration of gravity, M_L is the equivalent tower mass of the tower and rotor, and S_i and I_i represent the static moment and moment of inertia of the ith blade about the lag hinge.

The mechanical stability of this rotor-tower system can be found by neglecting gravity and blade unbalance forces (g = 0, S_i = const), and introducing the multiblade coordinate transformation

$$\phi_i = a(t) \sin\psi_i + b(t) \cos\psi_i \qquad (3)$$

This eliminates all the periodic coefficients in Eqs. (2) for $N \geqslant 3$, and the stability of the resulting equations in q_L, a, b, can be investigated in the standard manner. Figure 3 shows the results for a typical 3-bladed rotor with varying amounts of critical damping ratio ζ_i in the tower and in the blades. In general adding damping stabilizes the system, but under certain circumstances, the addition of unequal amounts of damping can destabilize the system from the no damping case. For a 2-bladed rotor, effects are similar, but with additional small instability regions.

Effects of small, static unbalance can be found by assuming that $S_1 = S + \Delta S$, $S_2 = S_3 = \ldots = S$. The right hand side of Eqs. (2) then reduces to the forcing function $\Omega^2 S \sin \Omega t$. By neglecting the small ΔS variations in the periodic coefficients, and introducing again the multiblade coordinate transformation, Eq.(3), the basic equations reduce to the forced harmonic response of a conventional spring mass system involving the coordinates q_L, a, b. The resulting tower and rotor responses become

$$q_L(t) = q_{LS} \sin\Omega t + q_{LC} \cos\Omega t$$

$$\phi_1(t) = \frac{b_c + a_s}{2} + \left(\frac{b_s + a_c}{2}\right) \sin 2\Omega t + \left(\frac{b_c - a_s}{2}\right) \cos 2\Omega t \qquad (4)$$

where a_s, a_c, b_s, b_c are the sine and cosine responses of the coordinates, a, b. Figure 4 shows the amplitude of the blade lagging response ϕ_1 for a typical case. It is seen that strong 2/rev resonance responses occur in the blade when the rotation speed Ω equals 1/2 the lagging natural frequency ω_ϕ or when Ω equals the tower natural frequency ω_L. Adding damping to the blade or to the tower reduces the respective amplitude accordingly.

The effects of gravity loading can similarly be investigated by examining Eqs.(2). Generally, gravity acts directly on each blade without much tower interaction. Strong 1/rev resonances may occur when Ω equals the lagging frequency ω_ϕ and weak .5/rev parametric resonances may possibly occur when Ω equals twice ω_ϕ.

More comprehensive rotor-tower interactions were investigated by including the tower yawing motions (θ_x) and the blade flapping motions (β) in the previous analyses. The mechanical instability regions occurred at slightly lower rotation speeds Ω than before, but the general mechanisms were not changed significantly. These additional degrees of freedom

also affected somewhat the static unbalance loads. Of more significance was the direct effect of wind shear and tower shadow on the blade flapping loads when these additional motions were introduced. The investigation of these mechanical vibrations are continuing.

REFERENCES

1. Miller, R.H., et al., "Wind Energy Conversion," Final Report, ERDA/NSF-00826/75-3, M.I.T. Aeroelastic and Structures Research Laboratory Report ASRL TR 184-3, October 1976.

2. Quarterly Progress Report, "Wind Energy Conversion," October-December 1976, COO-4131/76/1, M.I.T. Aeroelastic and Structures Research Laboratory Report ASRL TR 184-4, January 1977.

3. Quarterly Progress Report, "Wind Energy Conversion," January-March 1977, COO-4131/77/1, M.I.T. Aeroelastic and Structures Research Laboratory Report ASRL TR 184-5, April 1977.

4. Quarterly Progress Report, "Wind Energy Conversion," April-June 1977, COO-4131/77/2, M.I.T. Aeroelastic and Structures Research Laboratory Report ASRL TR 184-6, July 1977.

5. Chopra, I., "Nonlinear Dynamic Response of Wind Turbine Rotor," Ph.D. Thesis, Department of Aeronautics and Astronautics, M.I.T., Cambridge, Mass., February 1977.

DISCUSSION

Q. Comment: It is the flywheel resonance and mechanical instability problems that have primarily dictated natural frequencies of the tower well above the operating range of the rotor.

A. Yes. These factors play important roles, together with the forced vibrations due to rotor static unbalance, gravity loads, and air loads. Generally, I believe, to avoid significant "ground resonance" type mechanical instability, the blade lagging frequency (in-plane vibrations) would need to be above the rotation speed of the rotor. Low natural frequencies of the tower usually give rise to large forced vibration as the rotor speed passes through the tower natural frequency (and also through one half the tower natural frequency for two bladed rotors).
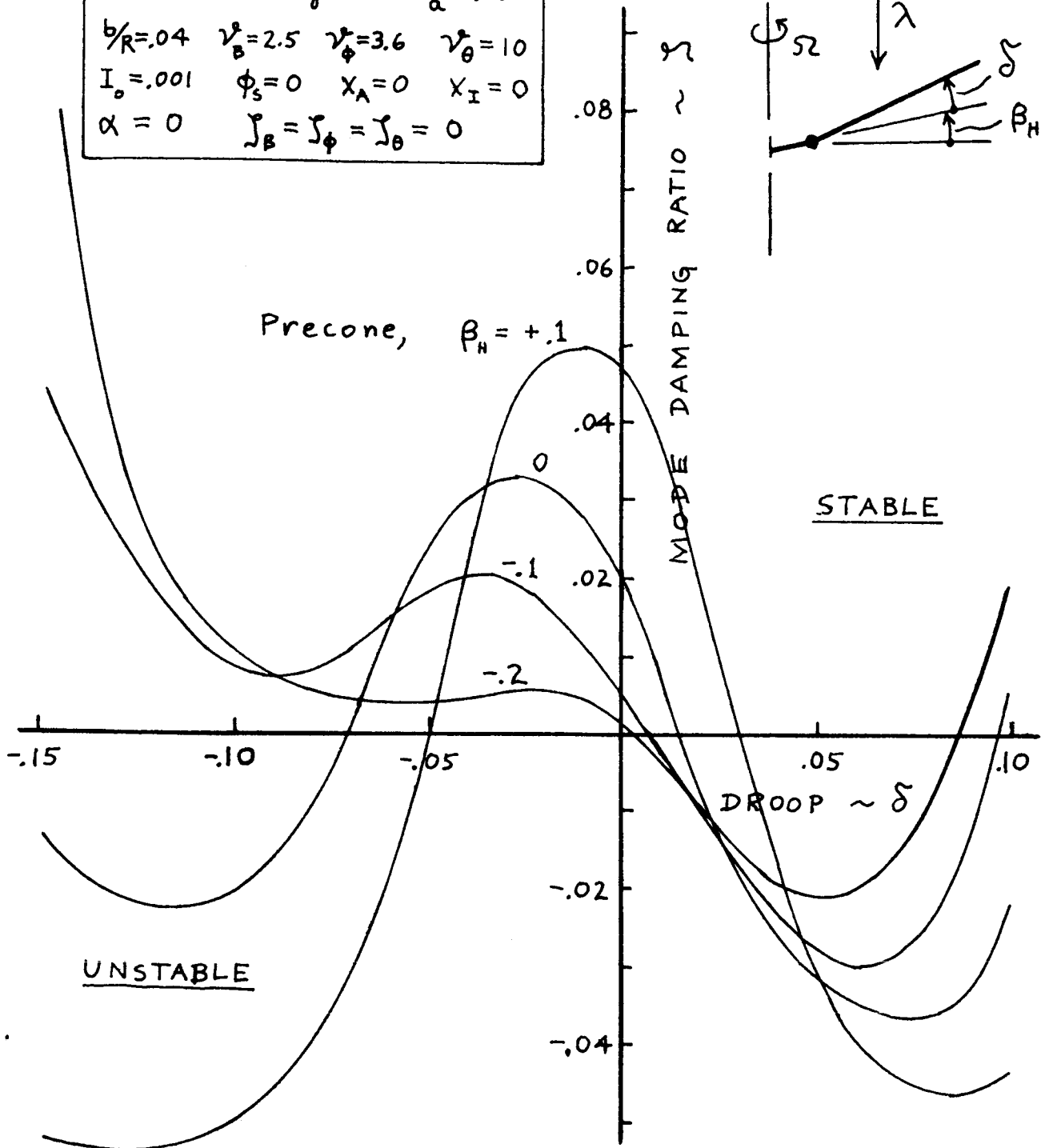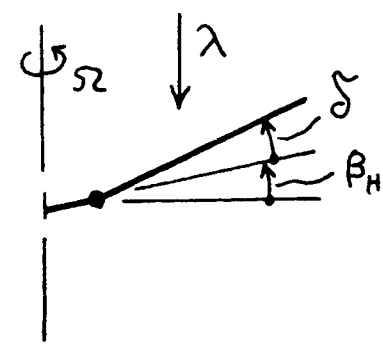
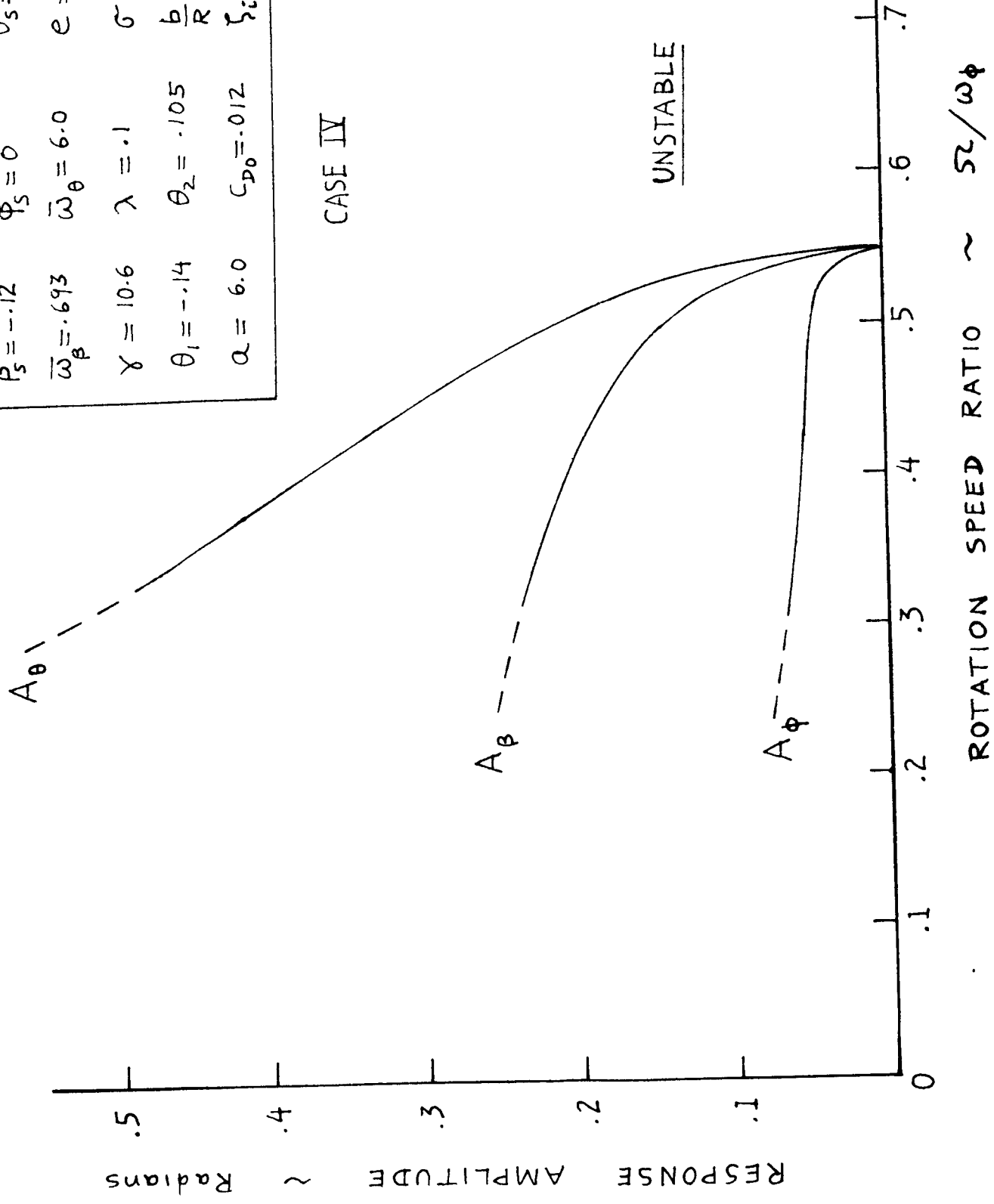Figure 1 - Effect of precone and droop on aeroelastic stability of lag mode.

Figure 2. - Flutter solution (nonlinear limit cycles).

58
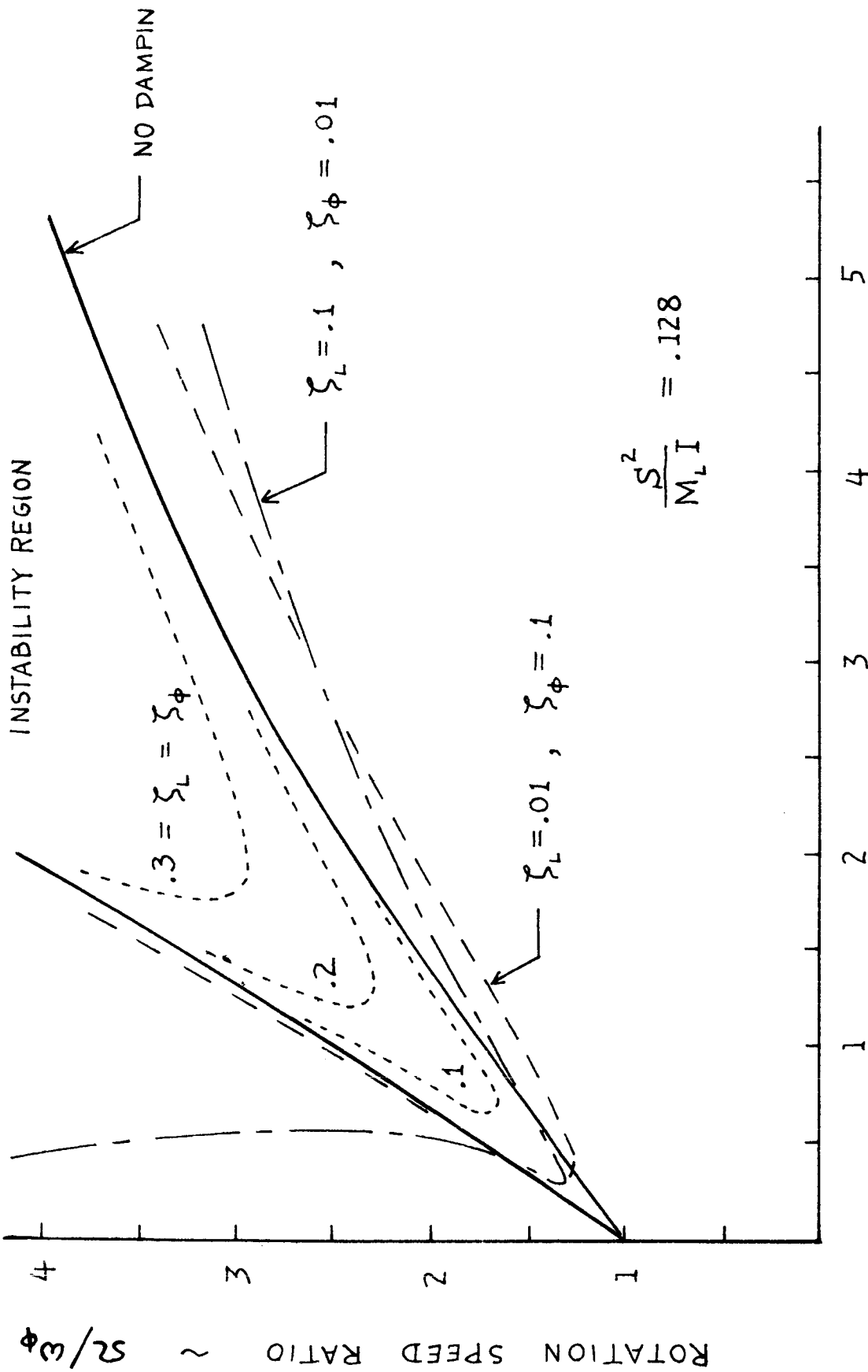
Figure 3. - Mechanical instability regions for a three-bladed rotor.

$$\frac{S^2}{M_L I} = .128$$

TOWER TO LAG FREQUENCY RATIO $\sim \omega_L/\omega_\phi$

ROTATION SPEED RATIO $\sim \Omega/\omega_\phi$

INSTABILITY REGION

NO DAMPIN

$\zeta_L = .1 \ , \ \zeta_\phi = .01$

$.3 = \zeta_L = \zeta_\phi$
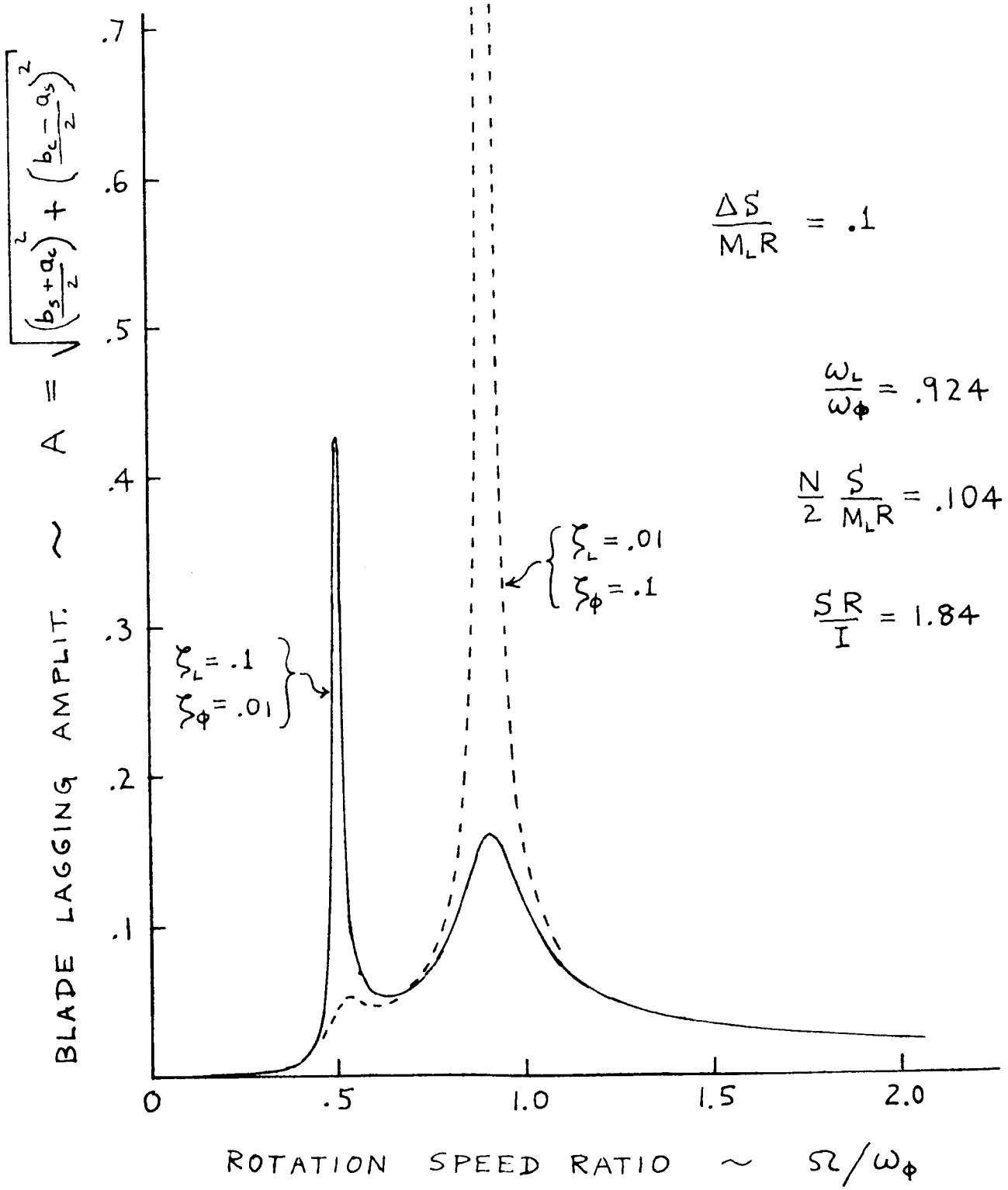
$\zeta_L = .01 \ , \ \zeta_\phi = .1$

59

Figure 4. - Forced response of rotor to static unbalance.